Glycolipid Nanotube Hollow Cylinders as Substrates: Fabrication of One-Dimensional Metallic−Organic Nanocomposites and Metal Nanowires

Bo Yang,[†] Shoko Kamiya,[‡] Yoshiki Shimizu,[†] Naoto Koshizaki,[†] and Toshimi Shimizu*,[†,‡]

Nanoarchitectonics Research Center, National Institute of Advanced Industrial Science and Technology (AIST), Tsukuba Central 5, 1-1-1 Higashi, Tsukuba, Ibaraki 305-8565, Japan, and CREST, Japan Science and Technology Agency (JST), Tsukuba Central 4, 1-1-1 Higashi, Tsukuba, Ibaraki 305-8562, Japan

Received February 26, 2004. Revised Manuscript Received May 1, 2004

A synthetic glycolipid *N*-(11-*cis*-octadecennoyl)-*β*-D-glucopyranosylamine was employed for the fabrication of organic tubular structures with a cyclic hollow cylinder 30−50 nm wide through molecular self-assembly in water. Gold or silver nanoparticles encapsulated in the hollow cylinders of the lipid nanotubes (LNTs), GNPs@LNT or SNPs@LNT, respectively, were fabricated by loading aqueous gold (GNPs) or silver nanoparticles (SNPs) into the LNT hollow cylinders using capillary force. To explore an advanced fabrication method for one-dimensional organization of metals, we have removed the LNT organic shell of the GNPs@LNT or SNPs@LNT nanocomposite by firing the nanocomposite in air at 450−1000 °C. A continuous gold nanowire 20−30 nm wide was successfully obtained under the firing conditions of $T = 550-750$ °C, indicating that the inner cavity of the LNT can also be used as a template for the organization of gold nanowire. On the other hand, we have found no remarkable formation of silver nanowires after the same treatment for the SNPs@LNT nanocomposite as mentioned for the GNPs@LNT. All the nanostructures have been analyzed using transmission electron microscopy (TEM), field emission scanning electron microscopy (FE-SEM), energy-dispersive X-ray analysis (EDXA), and selected area electron diffraction (SAED).

Introduction

There has been growing interest in the fabrication of metallic−organic nanocomposites consisting of naturally occurring biomaterials and metal nanoparticles for advanced materials applications.[1−4] In particular, the fabrication of one-dimensional (1-D) morphology for nanocomposite including cylinders, tubes, and wires is of great importance because the unique properties of nanotubes and nanowires, such as high dielectric constant, controlled release, and magnetic function, can provide the possibility to lead to real world applications.[5−9] One possible approach toward such nanostructures is to use biomolecular templates. For example, DNA molecules have been used as templates to fabricate a metal nanowire,[10−12] whereas tobacco mosaic virus (TMV)[13−16] and protein microtubules[17] were used to prepare high aspect ratio nanotubular composites through template-directed metallization. On the other hand, synthetic biomaterials, such as lipid nanotubes,[1f,g,6b,18−20]

* Corresponding author. Telephone: +81-29-861-4544. Fax: +81-29-861-4545. E-mail: tshmz-shimizu@aist.go.jp.

[†] National Institute of Advanced Industrial Science and Technology.

[‡] Japan Science and Technology Agency.

(1) (a) *Biomimetic Materials Chemistry*; Mann. S., Ed.; VCH: New York, 1996. (b) Wong, K. K. W.; Douglas, T.; Gider, S.; Awschalom, D. D.; Mann, S. *Chem. Mater.* **1998**, *10*, 279. (c) Wong, K. K. W.; Mann, S. *Adv. Mater.* **1996**, *8*, 928. (d) Shenton, W.; Pum, D.; Sleytr, U.; Mann, S. *Nature* **1997**, *389*, 585. (e) Davis, S. A.; Burkett, S. L.; Mendelson, N. H.; Mann, S. *Nature* **1997**, *385*, 420. (f) Archibald, D. D.; Mann, S. *Nature* **1993**, *364*, 430. (g) Burkett, S. L.; Mann, S. *Chem. Commun.* **1996**, 321. (h) Dujardin, E.; Mann, S. *Adv. Mater.* **2002**, *14*, 775.

(2) Douglas, T.; Young, M. *Nature* **1998**, *393*, 152.

(3) Baral, S.; Schoen, P. *Chem. Mater.* **1993**, *5*, 145.

(4) Niemeyer, C. M. *Angew. Chem. Int. Ed.* **2001**, *40*, 4128;

(5) Special section, "Engineering a Small World" *Science* **1991**, *254*, 1300.

(6) (a) Schnur, J. M.; Price, R.; Schoen, P. E.; Yager, P.; Calvert, J. M.; Geoger, J.; Singh, A. *Thim Solid Films* **1987**, *152*, 181. (b) Schnur, J. M. *Science* **1993**, *262*, 1669.

(7) Price, R.; Patchan, M. *J. Microencapsulation* **1991**, *8*, 36.

(8) Burke, T. G.; Singh, A.; Yager, P. *Ann. N. Y. Acad. Sci.* **1987**, *507*, 330.

(9) Cui, Y.; Wei, Q. Q.; Park, H. K.; Lieber, C. M. *Science* **2001**, *293*, 1289.

(10) Braun, E.; Eichen, Y.; Sivan, U.; Ben-Yoseph, G. *Nature* **1998**, *391*, 775.

(11) Ford, W. E.; Harnack, O.; Yasuda, A.; Wessels, J. M. *Adv. Mater.* **2001**, *13*, 1793.

(12) Richter, J.; Seidel, R.; Kirsch, R.; Mertig, M.; Pompe, W.; Plaschke, J.; Schackert, H. K. *Adv. Mater.* **2000**, *12*, 507.

(13) Dujardin, E.; Peet, C.; Stubbs, G.; Culver, J. N.; Mann, S. *Nano Lett.* **2003**, *3*, 413.

(14) (a) Knez, M.; Sumer, M.; Bittner, A. M.; Wege, C.; Jeske, H.; Kooi, S.; Burghard, M.; Kern, K. *J. Electroanal. Chem.* **2002**, *522*, 70. (b) Knez, M.; Bittner, A. M.; Boes, F.; Wege, C.; Jeske, H.; Maiss, E.; Kern, K. *Nano Lett.* **2003**, *3*, 1079.

(15) Mertig, M.; Kirsch, R.; Pompe, W.; Engelhardt, H. *Eur. Phys. J.* **1999**, *9*, 45.

(16) Shenton, W.; Douglas, T.; Young, M.; Stubbs, G.; Mann, S. *Adv. Mater.* **1999**, *11*, 253.

(17) Boal, A. K.; Headley, T. J.; Tissot, R. G.; Bunker, B. C. *Adv. Funct. Mater.* **2004**, *14*, 19.

(18) Zabetakis, D. *J. Mater. Res.* **2000**, *15*, 2368.

(19) (a) Letellier, D.; Cabuil, V. *Prog. Colloid Polym. Sci.* **2001**, *118*, 248. (b) Letellier, D.; Sandre, O.; Ménager, C.; Cabuil, V.; Lavergne, M. *Mater. Sci. Eng. C.* **1997**, *5*, 153.

10.1021/cm049695j CCC: $27.50
Published on Web 06/15/2004

Scheme 1. Molecular Structure of the Glycolipid 1 Self-Assembling into Lipid Nanotubes (LNTs)

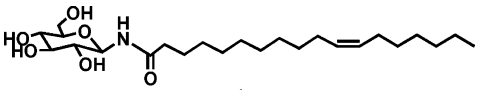

1

peptide nanotubes,[21] and nanofibrils[22] have also been exquisitely used to direct the nucleation, deposition, and assembly of metal nanoparticles. The reason for the use of the organic templates is that they possess well-defined morphologies, unique nanometer-sized dimensions, functionally controllable inner and outer surfaces, and possibility for large-scale production. However, most of these approaches, to the best of our knowledge, have focused on using the outer surfaces of the templates, except for the TMV template by Dujardin et al.[13] and diacetylenic phohpholipid tubules by Letellier et al.[19b] We have recently developed the capability to introduce $HAuCl_4$ aqueous solutions into a vacant hollow cylinder (50−80 nm inner diameters) of a synthetic glycolipid nanotube (LNT) by capillary force and succeeded in subsequent photoreduction of Au(III) into Au(0) in a "ship-in-bottle" fashion, using the hollow cylinder as a nanoflask.[23] Thus, we have obtained a unique metallic−organic tubular nanocomposite, in which gold nanoparticles 5−10 nm wide are filling the core of the hollow cylinder of the LNT. However, there have been two limitations for the use of this intriguing method for the fabrication of the 1-D metallic−organic nanostructures: This methodology is only applicable to a photoreducible solution system for the nanoparticle deposition. Second, the size control of the resultant metal nanoparticles is unattainable.

Metal colloid nanoparticles are known to have both well-defined shapes and controllable size dimensions, being easily available for a variety of metals. Here we describe the fabrication of advanced 1-D metallic−organic nanocomposites by loading a vacant LNT hollow cylinder with water-soluble gold (GNPs) and silver nanoparticles (SNPs) using capillary force. Furthermore, we attempted to fabricate a gold or silver nanowire by utilizing a firing process to remove the LNT organic outer shell from the gold or silver nanoparticle-encapsulated LNT (GNPs@LNT or SNPs@LNT, respectively) nanocomposite.

Experimental Section

Materials. A glycolipid *N*-(11-*cis*-octadecenoyl)-β-D-glucopyranosylamine **1** (Scheme 1) was synthesized as described previously.[23] Hydrogen tetrachloroaurate(III) trihydrate ($HAuCl_4 \cdot 3H_2O$, 99.9+%), silver nitrate ($AgNO_3$, 99.0+%), sodium borohydride ($NaBH_4$, 99%), and trisodium citrate dihydrate (99%) were all purchased from Aldrich. Glutathione (reduced form, 97%) and other organic chemicals of analytical reagent grade were supplied from Wako Pure Chemical Industry. Water used in all the experiments was purified through a Milli-RX12α system (Millipore, Co., Ltd.).

Preparation of Self-Assembled LNTs. In this paper, we used glycolipid nanotubes that were derived by the self-assembly of glycolipid **1** in water. In a typical procedure, glycolipid **1** (1 mg) was dissolved in methanol (1 mL), and the solution was evaporated in a round-bottomed flask by rotating it, and a lipid thin film was then formed on the glass wall. Pure water (20 mL) was then added to the flask and the mixture was sonicated at room temperature for 1 h (Branson 1200, 60 W, Yamato Co., Ltd.). After sonication, the aqueous dispersion was heated in an oil bath at 100 °C for 1 h. Then, the obtained transparent dispersion was allowed to cool slowly to room temperature over a period of 48−72 h. A white suspension of nanotubes was obtained.

Synthesis of GNPs and SNPs. Three different types of GNPs in average diameters have been used in this study. Relatively smaller sized GNPs (diameter 1−3 nm) were prepared by a single-phase method using glutathione as a stabilizer.[24] For a typical procedure, hydrogen tetrachloroaurate trihydrate (200 mg) and glutathione (156 mg) were dissolved in methanol (30 mL). To the mixture was added acetic acid (5 mL) to prevent the deprotonation of glutathione. A freshly prepared aqueous solution (15 mL) of sodium borohydride (378 mg) was added carefully with vigorous stirring. The solution turned brown in color immediately, indicating the formation of gold clusters in the size range of 2.5 ± 0.5 nm. After stirring for 40 min further the solvent was removed under reduced pressure. To remove excess borates, acetates, and glutathione, we purified the dark-brown solid by dialysis against water for 5 days using a cellulose ester tube (cutoff molecular weight 3000). After the dialysis the water was removed under reduced pressure to give the pure product as a dark-brown solid.

Relatively larger sized GNPs (diameter: 15−20 nm or > 50 nm) were synthesized by the sodium citrate reduction method.[25] Briefly, 0.01% (w/w) hydrogen tetrachloroaurate trihydrate solution (95 mL) was heated to boiling, to which a given volume (5 and 1 mL for 15- and 50-nm gold particle, respectively) of 1% sodium citrate solution was added with thorough stirring. The solution was boiled for 30 min and cooled to room temperature. The GNPs were purified by dialysis in the same manner as described above.

Unless otherwise noted, relatively smaller sized SNPs (<4 nm) were prepared by a method similar to that of the GNPs as described above. In the case of SNPs, 100 mg of silver nitrate was used. We used only the small SNPs in this study.

Preparation of GNPs@LNT and SNPs@LNT Nanocomposites. The GNPs@LNT or SNPs@LNT nanocomposites were prepared by introducing the aqueous solution of GNPs or SNPs into the LNT hollow cylinder using capillary action as shown schematically in Figure 1. First, the LNTs were dried by lyophilization to remove the filled water in the LNT core (step 1). For a typical procedure, an aqueous dispersion (20 mL) containing 1 mg of the LNT was added in a glass test tube and put in liquid nitrogen for 10 min. The frozen sample was transferred into a freeze-dryer (Eyela FD-1000, Tokyo Rikakikai Co., Ltd.) and dried for 72 h at vacuum (1.0 Pa) to remove the remaining water completely. Then, we put the lyophilized LNT powder onto the aqueous solution of GNPs or SNPs and stirred it slowly for 12 h (step 2). This treatment enables the GNPs or SNPs to fill the LNTs by capillary action. The filled LNTs were separated by centrifugation at 5000 rpm for 30 min and washed thoroughly with pure water five times.

Preparation of Gold and Silver Nanowire. The aqueous dispersion containing GNPs@LNT or SNPs@LNT nanocomposite was drop on a clear mica sheet and dried in air at room temperature for 24 h. The mica sheet was put in an oven and heated in air at 450−1000 °C for 40 min to completely remove the organic LNT template (Figure 1, step 3).

(20) Kirsch, R.; Mertig, M.; Pompe, W.; Wahl, R.; Sadowski, G.; Bohm, K.-J.; Unger, E. *Thin Solid Films.* **1997**, *305*, 248.
(21) Djalali, R.; Chen, Y. F.; Matsui, H. *J. Am. Chem Soc.* **2002**, *124*, 13660.
(22) Fu, X.; Wang, Y.; Huang, L.; Sha, Y.; Gui, L.; Lai, L.; Tang, Y. *Adv. Mater.* **2003**, *11*, 902.
(23) Yang, B.; Kamiya, S.; Yoshida, K.; Shimizu, T. *Chem. Commun.* **2004**, 500−501.
(24) Brust, M.; Fink, J.; Bethell, D.; Schiffrin, D. J.; Kiely, C. *J. Chem. Soc. Chem. Commun.* **1995**, 1655.
(25) Diff, D. G.; Curtis, A. C.; Edwards, P. P.; Jefferson, D. A.; Johnson, B. F. G.; Logan, D. E. *Angew. Chem. Int. Ed. Engl.* **1987**, *26*, 676.

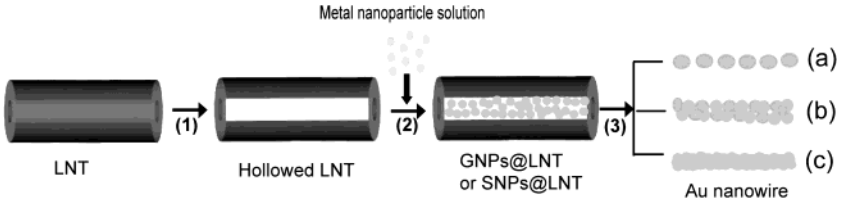

Figure 1. Schematic diagram for the fabrication of GNPs@LNT or SNPs@LNT and a gold nanowire. (1) Lyophilization of LNTs to empty the internal hollow volume, (2) filling LNTs with aqueous solution containing metal (Au or Ag) nanoparticles, and (3) removing the LNT shell by firing process. (a) discrete and (b, c) continuous gold nanowires.

Characterization. The morphology and size dimension of the LNTs, metal nanoparticles, and metallic−organic nanocomposites were characterized by TEM and FE-SEM. Samples for TEM were prepared by putting a drop of sample solution on a carbon-coated copper grid, and dried in a vacuum at room temperature overnight. TEM observation and electron diffraction were carried out using a JEM-2000X (JEOL) microscopy operated at 200 kV and equipped with an energy-dispersive X-ray analyzer (EDXA, Genesis spectrum, EDXA, Inc.). A sample of the LNTs for FE-SEM (S-4800, Hitachi) were prepared by mounting the solution of the LNT on an alumina specimen mount and dried in a vacuum at room temperature.

Results and Discussion

Glycolipid Nanotube. Over the last two decades, several research groups have developed the synthesis and application of LNTs[6b,26−29]since the first reports on lipid tubule formation by Yager et al.,[30] Ihara et al.,[31] and Nakashima et al.[32] To date we have focused on synthetic glycolipids as potential molecular building blocks self-assembling into LNTs with 100% efficiency[29b−d] and recently explored a newly optimized glycolipid, *N*-(11-*cis*-octadecenoyl)-*β*-D-glucopyranosylamine **1** (Scheme 1). The lipid **1** can self-assemble in water to produce monodispersed and well-defined LNTs in approximately 100% yields. Typical FE-SEM and TEM images of the LNTs from **1** are shown in Figure 2. The FE-SEM picture (Figure 2a) shows that the LNTs have a straight shape with lengths ranging from several tens to hundreds of microns. The distribution of outer diameter for the LNTs proved to be very narrow (∼200 nm). High-magnification images of TEM (Figure 2b) and FE-SEM (Figure 2c) clearly display that the LNTs possess a hollow cylinder inside, opening on both ends. The inner diameters of the LNTs range from 30 to 50 nm. The thickness of the LNT wall membrane is approximately 80 nm, suggesting the presence of several tens of bilayers. To get insight into the thickness of a single lipid bilayer, we carried out powder X-ray diffraction (XRD) measurement for the LNTs. The diffraction patterns of the LNTs show a Bragg peak of lamellar

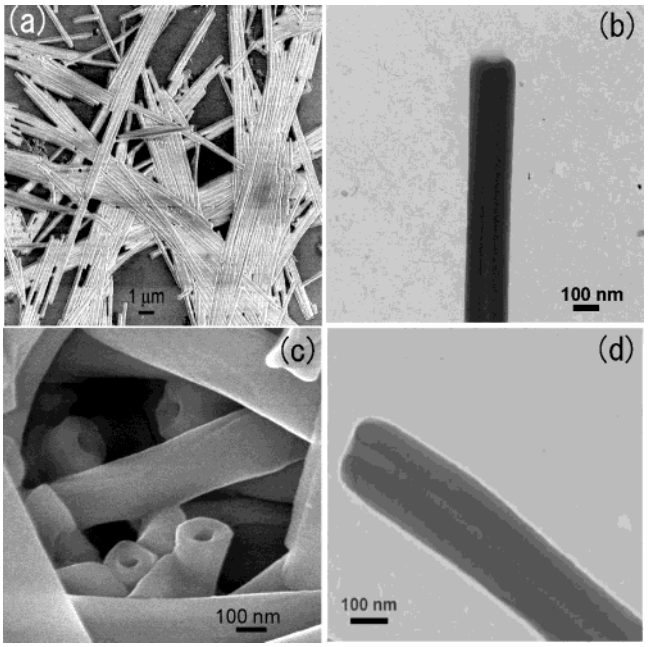

Figure 2. Electron microscopic images of LNTs (a, b) before and (c, d) after the lyophilization treatment: (a, c) FE-SEM and (b, d) TEM images.

organization, and the evaluated *d* spacing was 4.8 nm. Therefore, the membrane wall of the LNT is found to consist of approximately 16 bilayers. This relatively thick wall of the LNT allows it to provide a mechanically stable structure with the LNTs upon lyophilization. Parts c and d of Figure 2 display the morphology of the LNTs after the lyophilization treatment, observed using FE-SEM and TEM, respectively. The two pictures clearly indicated that the hollow interiors of these open-ended LNTs remain almost intact as compared with those before the lyophilization treatment. Thus, we confirmed that the present LNTs can keep their tubular structures without any destruction, even after the lyophilization treatment.

GNPs and SNPs. Pure products of the smaller sized GNPs and SNPs are dark-brown solids and have a high solubility in water (over 50 mg/mL). The aqueous solution of GNPs or SNPs is thermally stable under laboratory conditions (room temperature and room light). TEM observation revealed that no remarkable change in the particle size was found over 6 months. Furthermore, each aqueous solution of the GNPs or SNPs gave no obvious surface plasmon absorptions around 520 nm in UV−visible absorption spectra, indicating that the particle sizes of the GNPs or SNPs are smaller than 4 nm.[33,34] Parts a and b of Figure 3 display TEM images for the obtained GNPs and SNPs, respectively. As can be seen in Figure 3a, relatively

(26) Thomas, B. N.; Safinya, C. R.; Plano, R. J.; Clark, N. A. *Science* **1995**, *267*, 1635.
(27) Fuhrhop, J.-H.; Koening, J. *Membranes and molecular assemblies: The Synkinetic Approach*; The Royal Society of Chemistry: Cambridge, 1994.
(28) Giulieri, F.; Guillod, F.; Greiner, J.; Krafft, M.-P.; Riess, J. G. *Chem. Eur. J.* **1996**, *2*, 1335.
(29) (a) Shimizu, T.; Kogiso, M.; Masuda, M. *Nature* **1996**, *383*, 487. (b) John, G.; Masuda, M.; Okada, Y.; Yase, K.; Shimizu, T. *Adv. Mater.* **2001**, *13*, 715. (c) Jung, J. H.; John, G.; Yoshida, K.; Shimizu, T. *J. Am. Chem. Soc.* **2002**, *124*, 10674. (d) John, G.; Jung, J.-H.; Minamikawa, H.; Yoshida, K.; Shimizu, T. *Chem. Eur. J.* **2002**, *8*, 5494. (e) Shimizu, T. *Macromol. Rapid Commun.* **2002**, *23*, 311.
(30) Yager, P.; Schoen, P. *Mol. Cryst. Liq. Cryst.* **1984**, *106*, 371.
(31) Yamada, K.; Ihara, H.; Ide, T. *Chem. Lett.* **1984**, 1713.
(32) Nakashima, N.; Asakuma, S.; Kunitake, T. *J. Am. Chem. Soc.* **1985**, *107*, 509.

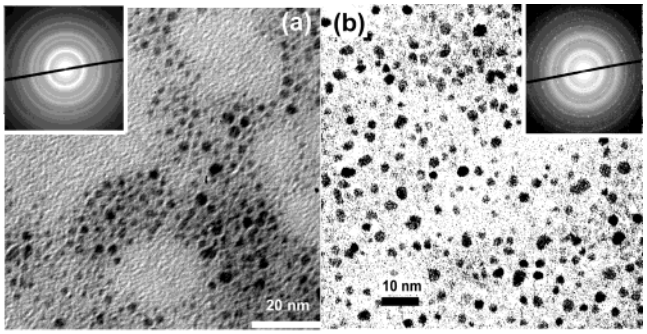

Figure 3. TEM images of (a) water-soluble gold nanoparticles (GNPs) and (b) water-soluble silver nanoparticles (SNPs).

uniform, spherical gold nanoparticles with diameters of 1−3 nm are obtainable. On the basis of the measurement for 500 particles in different image regions, the average size of the particles was estimated to be 2.5 nm. The selected area electron diffraction (SAED) pattern indicates a set of diffraction rings from gold that can be indexed to the [111], [200], [220], [311], and [222] reflections, suggesting the presence of face-centered cubic (fcc) polycrystalline structure of the GNPs (Figure 3a, inset). On the other hand, the SNPs produced a relatively monodispersed colloid system as compared with that of GNPs (Figure 3b). The average particle size was estimated to be 3 nm on the basis of measurement of 400 particles in different regions of the TEM picture. The SAED pattern (Figure 3b inset) recorded for the image of Figure 3b showed a diffusive ring pattern ascribable to the [111], [200], [220], [311], and [400] reflections from a well-ordered fcc structure of metallic silver.

Morphology and Structure of GNPs@LNT and SNPs@LNT Nanocomposites. As a reference experiment, we initially tried to add the GNPs into the aqueous dispersion containing water-filled LNTs and then stirred the mixture gently for 24 h at room temperature. However, the percentage of the obtained LNT encapsulating GNPs proved to be very low (<3%) under this condition. This finding means that only diffusion of the GNPs cannot allow them to penetrate into the water-filled LNTs in aqueous dispersion. Thus, we realized that the water volume filling the LNT cavity should be removed in advance to introduce the GNPs into the LNTs efficiently. Therefore, we removed the water in the LNTs core to obtain the nanotube hollow cylinder in a way similar to the method described previously[23] (step 1 in Figure 1). Second, capillary suction enabled the GNPs to penetrate into the hollow LNT interior, together with the aqueous solution (step 2 in Figure 1). Eventually, the yield of the LNTs encapsulating the GNPs increased to approximately 30% by using this method.

Figure 4a,b shows TEM images of a typical, 1-D metallic−organic nanocomposite (GNPs@LNT), where the LNT is encapsulating the GNPs obtained in this way. We can obviously observe dark contrast as a core, sheathed in the LNTs along the long axis, the diameter of which is approximately 30 nm, corresponding to that

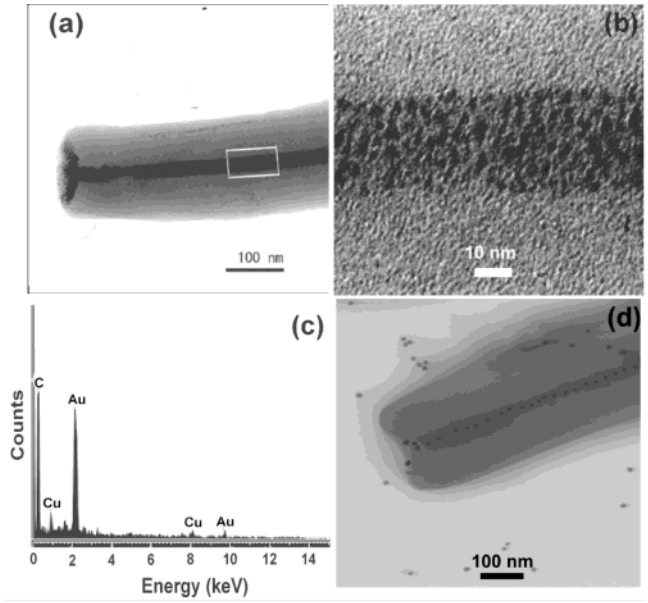

Figure 4. TEM images of LNTs encapsulating different sized gold nanoparticles. (a) Lower magnification and (b) higher magnification image showing that the 1−3 nm Au nanoparticles load the LNT hollow cavity. (c) EDXA spectrum of that from b showing the presence of gold. (d) Gold nanoparticles with diameters of 15−20 nm loading the LNT hollow cavity.

of the LNTs hollow cylinder (Figure 4a). This finding means that the hollow cavity of the LNTs loads the GNPs with high population. Furthermore, the observation at high magnification revealed that the diameters of the GNPs encapsulated are 1−3 nm wide (Figure 4b), similar to those in the GNPs solution (see Figure 3a). It should be noted that the GNPs organize one-dimensionally in the confined nanospace that can be provided by the LNT hollow cylinder. To ensure that the dark core originates from the confined GNPs in the GNPs@LNT nanocomposites, we employed the energy-dispersive X-ray analysis (EDXA). As shown in Figure 4c, measured for the selected area in Figure 4b, we can confirm the presence of gold in the nanocomposites (E = 2.12 and 9.71 keV, ascribable to Au Mα and Lα). The EDXA spectrum also showed signals of copper and carbon originating from the copper grid and the carbon of the LNTs, respectively.

To get further insight into the influence of metal particle size on the formation of GNPs@LNT nanocomposites, we used three kinds of particles with different diameters ranging from 1 to 50 nm as GNPs in the experiment. Consequently, we found that relatively smaller particles (diameter 1−3 nm) are favorable to filling the LNTs with close packing with a relatively high filling yield of 30%. When increasing the particle size to 15−20 nm, we found that the discrete GNPs are aligning along the long axis of the LNT hollow and the loading yield decreased to 10% (Figure 4d). When we used relatively larger GNPs having an average diameter of more than 50 nm, we found no LNTs encapsulating the GNPs, since the diameter of the LNT hollow core is 30−50 nm.

Next, we applied the similar procedure as described above for the preparation of a metallic−organic composite of SNPs@LNT, where the LNT is encapsulating the SNPs. Figure 5a shows a low-magnification TEM image of the obtained SNPs@LNT nanocomposites. The

(33) Zheng, J.; Petty, J. T.; Dickson, R. M. *J. Am. Chem. Soc.* **2003**, *125*, 1778.
(34) Crooks, R. M.; Zhao, M. Q.; Sun, L.; Chechik, V.; Yeung, L. K. *Acc. Chem. Res.* **2001**, *34*, 181.

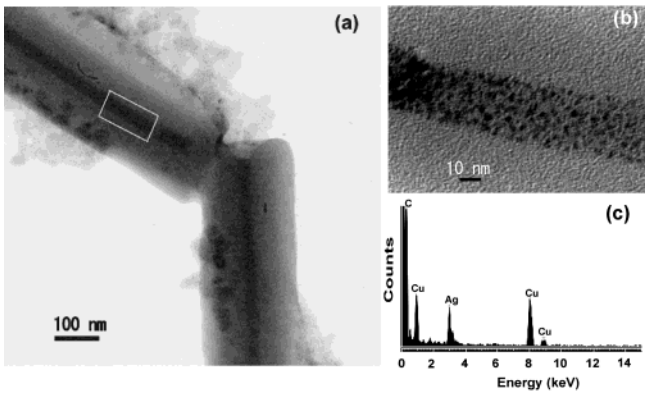

Figure 5. TEM images of LNTs loaded with silver nanoparticles. (a) Lower magnification and (b) higher magnification image showing that 2−4 nm silver nanoparticles load the LNT hollow cavity. (c) EDXA spectrum of that from b showing the presence of silver.

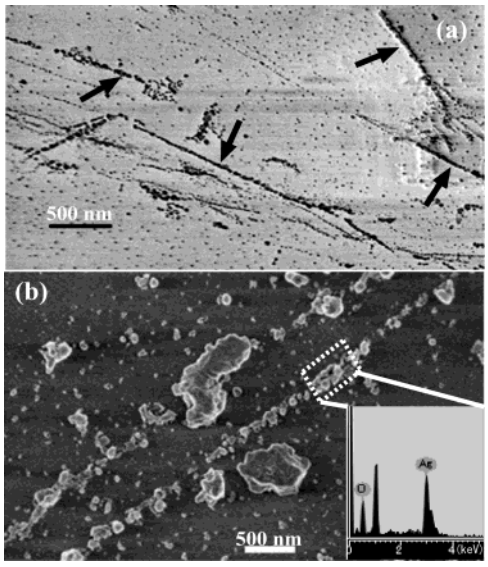

Figure 6. FE-SEM images of (a) gold and (b) silver nanoparticles with LNT nanocomposite after firing in air at 550 °C for 40 min. Insert: EDXA spectrum of a selected area.

hollow cavity of the LNTs displays relatively darker contrast as compared with that before loading, indicating the efficient loading of the SNPs into the LNTs. A high-magnification TEM image revealed that the spherical SNPs with diameters of 2−4 nm are organizing along the long axis of the LNTs hollow cavity (Figure 5b). EDXA spectra indicated the silver signal ascribable to Ag Lα at E = 2.98 keV (Figure 5c), evidencing the presence of a well-ordered fcc crystal structure of metallic silver.

Gold and Silver Nanowire. As described above, the GNPs or SNPs proved to be confined in the LNT hollow cylinder, organizing into high-axial ratio 1-D assemblies of the metal nanoparticles. This characteristic feature of the metallic−organic nanocomposites allows us to fabricate easily a metal nanowire by removal of the organic LNT shell through a firing process. Figure 6 shows the low-magnification FE-SEM images of the structure of metal nanowires after firing the GNPs@LNT or SNPs@LNT nanocomposites in air at 550 °C for 40 min. In Figure 6a we observed nanowire-like gold assemblies (diameter 20−30 nm) made of GNPs forming a line. On the other hand, no obvious silver nanowire was observed under the same condition, even though we can see one-dimensional alignment of nanoparticles (diameters: more than 100 nm) with irregular shapes. The EDXA spectrum (Figure 6b insert) showed a remarkably strong signal assignable to oxygen (E = 0.52 keV ascribable to O Kα), indicating that the SNPs were oxidized under the firing condition.

Therefore, we tried to use the organic solvent acetone to remove the LNT shell,[35] since the LNT can be dissolved in acetone solvent. This relatively milder method as compared with the firing process will cause no oxidation of the SNPs. However, we only observed random distribution of a lot of SNPs instead of nanowire structures. This means that there was not any strong attraction force between the particles, but the spatial confinement allows the organization of the SNPs in 1-D assemblies. The same treatment for the GNPs@LNT suggested that acetone would collapse the shape of the LNT template to disorder the 1-D assembly of metal nanoparticles. Thus, we realized that the metal nanoparticles should be confined stably in the LNT hollow cylinder during the firing process.

Application of the firing process for the GNPs@LNT nanocomposites seemed to be suitable for the fabrication of the gold nanowire. Complete removal of the LNT template can allow the GNPs confined in the LNT hollow to fuse into a 1-D metal nanowire upon firing (step 3 in Figure 1). The temperature condition is very critical for the efficient fabrication of homogeneous gold nanowire using the nanocomposites as a precursor. Thermogravimetric analysis (TGA) revealed that the decomposition of the LNT template starts at 293.6 °C because of the caramelization of the sugar moiety of the lipid, and the LNT template eventually burned out at 657.5 °C (see Supporting Information S1−S3). To optimize the temperature condition, we investigated the effect of firing temperatures on the change in the assembly state of the gold nanowire formed from the nanocomposites. Figure 7 shows the FE-SEM images of the gold nanowire obtained after firing at T = 450, 550, 750, and 1000 °C for 40 min. As can be seen in Figure 7a, many discrete gold nanowires and particles are observed at T = 450 °C, forming the random arrangement of relatively larger GNPs (diameter 20−30 nm) along a certain axis (Figure 1 step 3a). It should be noted here that nanometer-sized GNPs are found to have relatively lower melting points than bulk gold particles due to the enhanced mobility of gold atoms.[36,37] Buffat et al. reported on the reduction feature of the melting point of nanometer-sized gold particles as a function of decreasing particle size. Accordingly, the nanometer-sized GNPs (diameter 1−3 nm) used in this study on the substrate will melt at this temperature and convert into stable GNPs with larger diameters. Furthermore, somewhat imperfect fusion of GNPs was also observable in the discrete gold nanowire, indicating that the degree of fusion between GNPs is inhomogeneous.

(35) In a typical procedure, the suspension of the GNPs@LNT and SNPs@LNT nanocomposites was dropped on the TEM grid and dried at room temperature in a vacuum. Then, 50 μL of acetone was added on the grid three times to remove the LNTs. The washed grid was observed by TEM

(36) Buffat, P.; Borel, J. P. *Phys. Rew. A* **1976**, *13*, 2287.
(37) Ercolessi, F.; Andreoni, W.; Tosatti, E. *Phys. Rew. Lett.* **1991**, *66*, 911.

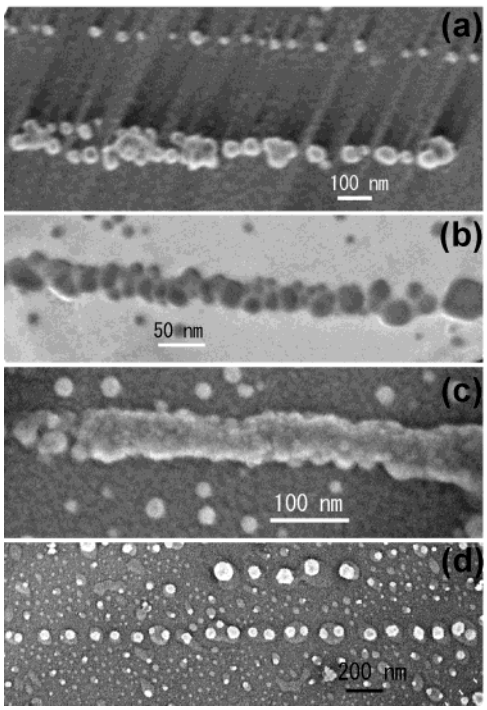

Figure 7. FE-SEM images of gold nanoparticles with LNT nanocomposite after firing in air at different temperatures for 40 min: (a) 450 °C, (b) 550 °C, (c) 750 °C, and (d) 1000 °C

Thus, we tried to optimize the degree of fusion of GNPs by varying the firing temperature. When increasing the temperature to 550 °C, we clearly observed the generation of continuous gold nanowires (Figure 1 step 3b). Figure 7b clearly indicated that the fusion between GNPs enables the formation of continuous gold nanowires. We found that increasing the firing temperature can increase the degree of fusion of gold particles. More interestingly, at 750 °C continuous polycrystalline gold nanowires (Figure 1 step 3c) were found to fuse into a single wire (Figure 7c). When the temperature is increased to 1000 °C, near to the melting point (1045 °C) of bulk gold, we found, however, no continuous gold nanowires (Figure 7d). The GNPs exist as a discrete spherical particle 50−100 nm wide. The interparticle distance between the gold particles also became larger than that at other temperatures (see Figure 7a−c). Relatively smaller GNPs will melt at this high temperature and convert into liquid drops on the substrate surface. These neighboring gold liquid drops will further unite into a single, larger gold drop within a certain distance.

Conclusion

We have achieved the fabrication of gold or silver nanoparticles encapsulated in the cylindrical hollow of the glycolipid nanotube with high-axial ratio by loading the vacant LNT hollow cylinder with aqueous gold or silver nanoparticles using capillary force. Aqueous gold or silver nanoparticles (1−3 nm wide) are favorable to form the GNPs@LNT or SNPs@LNT nanocomposite in relatively higher yields. This work will certainly lead to a simple and mild approach for the fabrication of a 1-D metallic−organic nanocomposite loading well-defined metallic colloid particles inside the organic nanotube hollow. In addition, the 1-D nanocomposite functions as a convergent template to fabricate a gold nanowire by removing the LNT shell through a firing process.

Acknowledgment. This work was supported by the Japan Society for the Promotion of Science (JSPS) Fellowship at the National Institute of Advanced Industrial Science and Technology (AIST), Tsukuba, Japan.

Supporting Information Available: Thermograms of the GNPs@LNT, the self-assembled LNT, and pure glycolipid **1** (PDF). This material is available free of charge via the Internet at http://pubs.acs.org.

CM049695J